Tellus (1994), 46A, 340–350
Printed in Belgium – all rights reserved

TELLUS
ISSN 0280–6495

A coupled ocean-atmosphere model of relevance to the ITCZ in the eastern Pacific

By SHANG-PING XIE[1]* and S. GEORGE H. PHILANDER, *Program in Atmospheric and Oceanic Sciences, Princeton University, Princeton, NJ 08544-0710, USA*

(Manuscript received 23 June 1993; in final form 10 February 1994)

ABSTRACT

The intertropical convergence zone (ITCZ) stays in the northern hemisphere over the Atlantic and eastern Pacific, even though the annual mean position of the sun is on the equator. To study some processes that contribute to this asymmetry about the equator, we use a two-dimensional model which neglects zonal variations and consists of an ocean model with a mixed layer coupled to a simple atmospheric model. In this coupled model, the atmosphere not only transports momentum into the ocean, but also directly affects sea surface temperature by means of wind stirring and surface latent heat flux. Under equatorially symmetric conditions, the model has, in addition to an equatorially symmetric solution, two asymmetric solutions with a single ITCZ that forms in only one hemisphere. Strong equatorial upwelling is essential for the asymmetry. Local oceanic turbulent processes involving vertical mixing and surface latent heat flux, which are dependent on wind speed, also contribute to the asymmetry.

1. Introduction

Solar radiation is the ultimate source of energy for motion in the atmosphere and oceans. The intertropical convergence zone (ITCZ), the ascending branch of the atmospheric Hadley cell in which a huge amount of latent heat is released, follows the seasonal migration of the sun in the zonal-mean sense. In the Atlantic and eastern Pacific sectors, however, it resides in the northern hemisphere throughout the year (Kornfield et al., 1967; Hubert et al., 1969; Mitchell and Wallace, 1992). The north–south asymmetry in the atmospheric circulation is associated with a corresponding one in the ocean: a zonally-oriented band of high sea surface temperature (SST) is collocated with the ITCZ to the north of the equator, while low SST is found at the same latitude in the southern hemisphere. In the boreal spring when the eastern equatorial Pacific warms up, two ITCZs are sometimes observed simultaneously in both hemispheres.

The reasons for the asymmetric climatic conditions in the eastern tropical Pacific and Atlantic seem related to geographic asymmetries, in the distribution of continents and in the orientation of coast lines for example. The purpose of the paper is not to explore such factors but to explore whether, in a world that has continental geometries perfectly symmetric about the equator, the ocean-atmospheric response to symmetric solar forcing can be asymmetric. Pike (1971) first investigated such a possibility and showed that a single ITCZ in one hemisphere is possible even when the SST is symmetric about the equator and has two off-equatorial maxima.

The focus of this paper is on the role of oceanic mixing process and surface evaporation in establishing asymmetries relative to the equator. In the eastern tropical Pacific, where the thermocline is shallow, wind-induced upwelling readily affects the sea surface temperature. This, however, can only happen in the presence of mixing processes

[1] Now at Joint Institute for the Study of the Atmosphere and Ocean, GJ-40, University of Washington, Seattle, WA 98195, USA.
* Corresponding author.

because the vertical velocity component vanishes at the surface. Thus, even though the tropical thermocline is particularly shallow near 10°N (because of the curl of the wind), sea surface temperatures there are at a maximum (Fig. 1), presumably because winds and thus mixing processes are weak near 10°N. This argument suggests that if the ITCZ is at a certain location, then it will tend to remain there because the low wind speeds at that location will ensure high sea surface temperatures there while the strong winds that converge onto the ITCZ will maintain low sea surface temperatures elsewhere. In other words, mixing processes and surface evaporation can contribute to the climatic asymmetries relative to the equator.

The purpose of this paper is to test this hypothesis by using a coupled ocean-atmosphere model. Our approach is to let all external conditions including solar radiation and geometry be equatorially symmetric and to see if the model develops asymmetric solutions. If the model has an asymmetric solution, we can then analyze the model result to determine the processes that maintain it. An annual cycle in SST is observed in the equatorial region, although the direct solar forcing has nearly zero annual component there. We will argue that the persistence of the ITCZ in the northern hemisphere contributes to this equatorial annual cycle in SST.

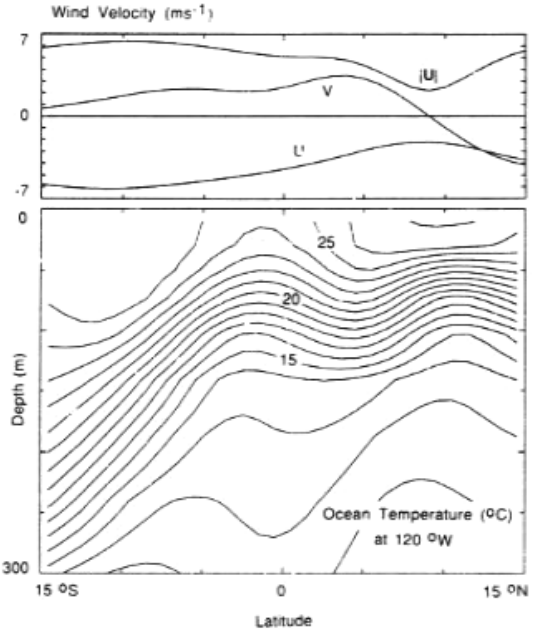

Fig. 1. Meridional section of annual-mean ocean temperature (from Levitus (1982) data set), and distribution of surface wind velocity (from Comprehensive Ocean-Atmospheric Data Set) along 120°W. The center of the ITCZ is where meridional wind vanishes.

The next section describes the coupled model. Sections 3 and 4 present the results from the standard and simplified models. Implications from this study are discussed in Section 5.

2. Model description

For simplicity, we use a 2-dimensional model that neglects variations in the zonal direction.

2.1. *Model atmosphere*

The model atmosphere is described by the equations

$$AU' - fV = 0, \tag{2.1}$$

$$AV + fU' = -\Phi_y, \tag{2.2}$$

$$A\Phi + C_a^2 V_y = -Q_a, \tag{2.3}$$

where (U', V) are the surface wind components, Φ is the geopotential difference between the ground and tropopause, A is the damping rate, f is the Coriolis parameter and C_a is the long gravity wave speed. Matsuno (1966) and Gill (1980) used such a model to study the atmospheric response to prescribed heating. Latent heat release in our model, Q_a, depends on sea surface temperature T in the following manner,

$$Q_a = K_Q(T - T_c)\, H(T - T_c), \tag{2.4}$$

where H is Heaviside's step function

$$H(x) = \begin{cases} 1, & \text{if } x \geqslant 0, \\ 0, & \text{otherwise.} \end{cases} \tag{2.5}$$

In (2.4), cumulus heating occurs only if $T > T_c = 27.5$°C. This choice is based on observations (Graham and Barnett, 1987). This empirical relation between SST and atmospheric heating sidesteps complicated problems related to water vapor. Friction in the surface boundary layer is presumably important in maintaining the low-level convergence in the ITCZ (Charney, 1969;

Wang and Li, 1992). A similar approach has been used in other studies with simple models (Anderson and McCreary, 1985; among others). This empirical approach is also consistent with GCM experiments with realistic boundary conditions, in which the ITCZ, with a narrow meridional extent, forms at the location of highest SST (Manabe et al., 1974).

Our zonally symmetric model lacks the eddy momentum transport and zonal SST (pressure) variation that maintain the easterly winds in the equatorial Pacific. To compensate these effects of nonlinearity and zonal asymmetry, we impose a spatially homogeneous easterly wind, U_{eq}. As a result, the zonal wind that forces the ocean is

$$U = U' + U_{eq}. \tag{2.6}$$

2.2. Model ocean

The motion of the upper ocean above the thermocline is assumed to be governed by the linear 1.5-layer reduced-gravity model equations,

$$(hu)_t - f(hv) = \tau_x/\rho - a(hu) + \nu(hu)_{yy}, \tag{2.7}$$

$$(hv)_t + f(hu) = -c^2 h_y + \tau_y/\rho - a(hv) + \nu(hv)_{yy}, \tag{2.8}$$

$$h_t + (hv)_y = -a(h - H), \tag{2.9}$$

where h, the depth of the thermocline, has an equilibrium value $H = 100$ m, hu is the mass transport from the surface to h, $c = (g'H)^{1/2}$ is the phase speed of long gravity wave with g' denoting the reduced gravity, ρ is the water density, a is the damping rate* and ν is the eddy viscosity coefficient. Nonlinear model calculations show that the meridional momentum advection terms are negligible. A linearized bulk formula is used to obtain the wind stress

$$(\tau_x, \tau_y) = C_D^*(U, V), \tag{2.10}$$

where, $C_D^* = \rho_a C_D U_0$ with ρ_a, C_D and U_0 being air density, drag coefficient and mean surface wind speed, respectively. Without a zonal pressure gradient to balance the wind stress at the equator in this zonally symmetric model, h sometimes can be negative because of strong equatorial upwelling. A device is then introduced to avoid negative h: h is adjusted to h_{min} if h becomes less than h_{min}. This device is technical rather than physical and has been used by Schopf and Cane (1983).

In the equatorial region, the bottom of the mixed layer coincides with the upper boundary of the thermocline. For simplicity, we use h as the depth of mixed layer. Then the temperature in the mixed layer, which is also the SST, can be obtained by solving the equation

$$\frac{\partial T}{\partial t} + v\frac{\partial T}{\partial y} = \frac{1}{h}\left(\frac{Q}{\rho c_p} - W_e \Delta T\right) + \kappa \frac{\partial^2 T}{\partial y^2}. \tag{2.11}$$

The rate for upper thermocline water to be entrained into the mixed layer is calculated using Kraus–Turner's formula (Kraus and Turner, 1967; Niiler and Kraus, 1977),

$$W_e \Delta T = \begin{cases} \dfrac{1}{h(1 - m_e \mathrm{Ri}^{-1})}\left(\dfrac{2mu_*^3}{\alpha g} - h\dfrac{Q}{\rho c_p}\right) \\ \qquad \text{if} \quad W_e > 0, \\ 0, \qquad \text{otherwise}, \end{cases} \tag{2.12}$$

where Ri is the Richardson number

$$\mathrm{Ri} = \frac{\alpha g \Delta T h}{|\Delta u|^2}. \tag{2.13}$$

In (2.11–13), Q is the surface heat flux, c_p is the specific heat at constant pressure, α is thermal expansion rate, ΔT and $|\Delta u|$ are the temperature jump and velocity shear across the bottom of the mixed layer, m (m_e) is non-dimensional and related to the efficiency at which turbulent kinetic energy generated by wind (vertical current shear) is used to entrain cold water and κ is the eddy diffusion coefficient. Of special importance here is the wind stirring term in which the air friction velocity u_* is proportional to the wind speed, i.e.,

$$u_* = \left(\frac{\tau}{\rho}\right)^{1/2} = \left(\frac{\rho_a}{\rho} C_D\right)^{1/2} |U|. \tag{2.14}$$

Equatorial turbulence observations indicate that the turbulent energy dissipation rate is proportional to u_*^3 (Moum and Caldwell, 1985; Herbert et al., 1991), consistent with (2.12). These observa-

* We use Rayleigh and Newtonian forms of damping instead of entrainment, feeling that the water entrained into the mixed layer does not come below the thermocline and would not affect its depth.

tions also show that turbulence in the upper ocean is especially high near the equator due to the strong vertical shear between the westward south equatorial current at the surface and the equatorial undercurrent. Since a 1.5 layer model cannot simulate the undercurrent, we simply specify the vertical shear in (2.12) as a time-invariant function that decays away from the equator,

$$\frac{m_e}{R_i} h = \frac{m_e}{\alpha g \Delta T} |\Delta u|^2 = h_e \exp\left[-\frac{1}{2}\left(\frac{y}{R}\right)^2 \right]. \quad (2.15)$$

The surface heat flux may be written as:

$$Q = Q_0 - L\rho_a C_E (1 - \mathrm{RH}) |U| q_s(T) = Q_0 - C_E^* |U| q_s(T), \quad (2.16)$$

where the second term on the rhs is latent heat flux, $C_E^* = L\rho_a(1 - \mathrm{RH}) C_E$ is the effective drag coefficient, L is the latent heat, RH is the relative humidity, and Q_0 represents the sum of shortwave and longwave radiation. Surface air temperature is closely related to SST and is assumed to be equal to SST here for simplicity. As a result, the sensible heat flux vanishes, which is observed to be very small compared to the latent heat flux in the tropics. The saturated moisture content q_s is given by the Clausius–Clapeyron equation

$$q_s(T) = q_0 \exp\left[\frac{L}{R_*}\left(\frac{1}{T_0} - \frac{1}{T}\right) \right], \quad (2.17)$$

where R_* is the gas constant for moist air and q_0 the saturated moisture content at the reference temperature T_0. We choose $T_0 = 30°\mathrm{C}$, $q_0 = 2.6 \times 10^{-2}$. The wind speed is not allowed to fall below a minimum value $U_{\min}$ in calculating u_* and latent heat flux. The latter assumption parameterizes the effect of high-frequency atmospheric disturbances (Philander and Seigel, 1985).

Unless specifically stated, we will only consider the steady-state response of the model to the annual mean solar forcing. Under clear sky conditions, the shortwave and the longwave radiation fluxes are weak functions of SST. In this paper, the annual mean net radiation in the model monotonously decreases with latitude and is given by

$$Q_0 = C_E^* U_{\min} q_s(T^*), \quad (2.18)$$

where

$$T^* = T_e + \frac{(T_p - T_e)}{L_y^2} y^2 \quad (2.19)$$

is the equilibrium temperature of an ocean that is at rest and has zero diffusion. Atmospheric convection and circulation are strongly influenced by the spatial distribution of SST. In the eastern Pacific, high cloudiness associated with the deep convection of the ITCZ at 10°N reduces the shortwave radiation by 25 Wm^{-2} (Oberhuber, 1988), tending to damp the high SST there and hence the north–south asymmetry in SST. On the other hand, the relative humidity is also high at 10°N, another consequence of the deep convection. The relative humidity difference between 10°N and 10°S is about 5% (Wright, 1988). If other parameters are the same, this difference in the relative humidity can cause the latent heat flux at 10°N to be 25 Wm^{-2} smaller than that at 10°S. In other word, the effects of cloudiness and relative humidity on SST largely cancel each other. Furthermore, a sophisticated moist atmospheric model is needed in order to include these effects, which is beyond the scope of this study. Since the purpose of this study is to investigate the role of oceanic processes in the formation of the ITCZ, we will use a constant relative humidity of 80% and prescribe a radiation flux (2.18) that is symmetric about the equator and independent of the SST distribution.

The equations that describe the coupled model are solved on Arakawa's C-grid with (U', V) calculated on the same grid as v. The model ocean

Table 1. *Values of parameters*

A	$(2\ \mathrm{days})^{-1}$	ν	$4 \times 10^3\ \mathrm{m^2\ s^{-1}}$
C_a	$45\ \mathrm{ms^{-1}}$	κ	$2 \times 10^3\ \mathrm{m^2\ s^{-1}}$
ρ_a	$1.3\ \mathrm{kg\ m^{-1}}$	c	$1.4\ \mathrm{ms^{-1}}$
K_Q	$1.2 \times 10^{-2}\ \mathrm{m^2\ s^{-3}\ K^{-1}}$	ρ	$1.0 \times 10^3\ \mathrm{kg\ m^{-3}}$
T_c	27.5°C	c_p	$4 \times 10^3\ \mathrm{Jkg^{-1}\ K^{-1}}$
C_D	1.4×10^{-3}	α	$2 \times 10^{-4}\ \mathrm{K^{-1}}$
U_0	$5\ \mathrm{ms^{-1}}$	m	1.75
C_E	1.4×10^{-3}	$h_{\min}$	20 m
RH	80%	h_e	18 m
L	$2.5 \times 10^6\ \mathrm{Jkg^{-1}}$	R	3×10^5 m
R^*	$462\ \mathrm{Jkg^{-1}\ K^{-1}}$	T_e	35°C
U_{eq}	$-4\ \mathrm{ms^{-1}}$	T_p	22°C
$U_{\min}$	$4\ \mathrm{ms^{-1}}$	L_y	3×10^6 m
a	$(100\ \mathrm{days})^{-1}$		

has a domain of $|y| < 3000$ km with a grid size of 50 km. The atmosphere has the same resolution but has a larger domain of $|y| < 4500$ km. At the poleward boundaries, there is no flow and no heat flux into the ocean and no meridional flow into the atmosphere. The time step is one hour. The atmosphere is coupled to the ocean once a day. The values of parameters used are listed in Table 1, which are typical of the equatorial eastern Pacific. A three dimensional nonlinear version of the model has previously been used to study the interannual variations (Anderson and McCreary, 1985; Xie et al., 1989). Additional experiments showed that the model results are not sensitive to either spatial or temporal resolution.

3. Steady state solutions

Although the model is strictly symmetric about the equator, our numerical calculations yield three steady solutions; one symmetric solution with twin ITCZs, and two asymmetric solutions in which a single ITCZ forms in only one hemisphere.

Symmetric initial conditions lead to the symmetric solution shown in Fig. 2. Equatorial upwelling causes a shallow thermocline at the equator,

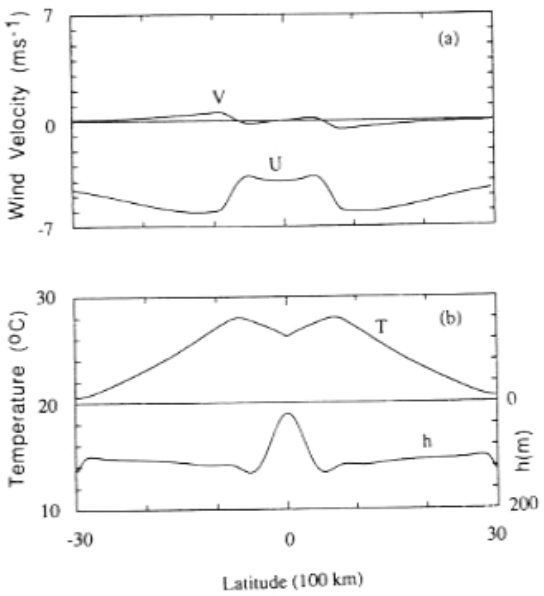

Fig. 2. Meridional distributions of (a) zonal and meridional wind velocities, and (b) SST and thermocline depth, in a symmetric solution.

where strong vertical mixing due to the shallow mixed layer and high current shear cools the surface water. The winds converge onto the off-equatorial regions where SST exceeds 27.5°C. Easterly trades prevail over the domain. This symmetric solution resembles the conditions of the eastern Pacific in spring when the SST contrast between the hemispheres is weak and when two ITCZs are sometimes observed.

An asymmetric initial condition, with such an SST profile that the SST greater than 27.5°C occurs only in the northern hemisphere, leads the model to an asymmetric steady state shown in Fig. 3. The SST distribution is quite realistic, with a minimum at the equator due to the equatorial upwelling. The maximum SST appears 800 km north of the equator, where the ITCZ forms. The meridional winds converge onto this ITCZ. South of the ITCZ southerly winds prevail. In the southern hemisphere the zonal winds induced by the southerlies intensify the easterly trades (see eq. (2.1)). In the northern hemisphere, on the other hand, the Coriolis force tends to turn the southerly flow eastward and thus weakens the easterlies. As a result, a strong contrast in total wind speed is generated across the equator (Fig. 3d). SST is high to the north of the equator where the winds are low, but is cooled down by strong winds to the south. Also plotted in Fig. 3d is T_E, the temperature obtained by eliminating the advection term in the SST equation. The difference between T and T_E reveals that the meridional current advection broadens the scale of the cold tongue. We will show in the next section that the latitude of the off-equatorial ITCZ is sensitive to the strength of equatorial upwelling. As in observations, the thermocline is shallow below the ITCZ (Fig. 3b), apparently because of the upward Ekman pumping induced by the positive curl of the zonal wind. By geostrophy, an eastward countercurrent exists south of this off-equatorial ridge. It has no effect on the SST in this two dimensional model. By symmetry, an asymmetric solution with the ITCZ in the southern hemisphere is also possible.

The SST maximum in the northern hemisphere is 3°C higher than that in the southern hemisphere in the model. At the location of the SST maxima, the effect of temperature advection vanishes so that the difference between the two off-equatorial SST maxima in Fig. 3d has to be explained by local

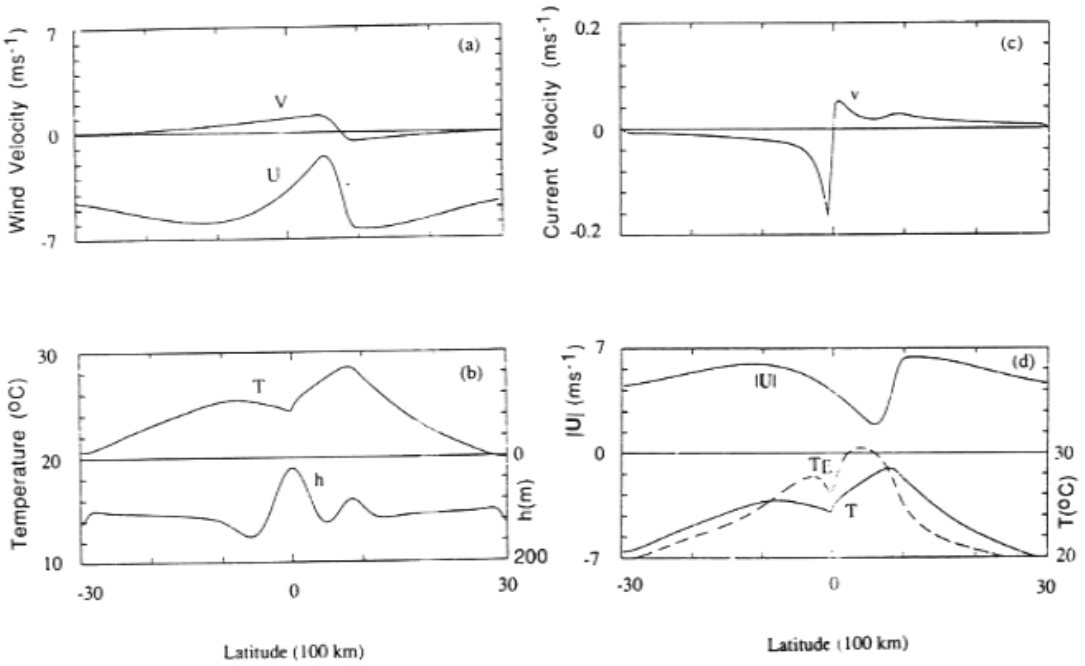

Fig. 3. Meridional distributions of (a) zonal and meridional wind velocities, (b) SST and thermocline depth, (c) meridional oceanic current velocity and (d) wind speed and equilibrium temperature in the absence of advection T_E (dashed line), in an asymmetric solution. SST is also plotted in (d) for comparison.

processes. Because the two maxima occur at similar latitudes, the solar radiation or Q_s does not account for this difference. The other two non-zero terms in the SST eq. (2.11) represent the effects of wind stirring and latent heat flux. We discuss these two effects separately in the rest of this section and Section 4.

To focus on the wind stirring process, we use a constant wind speed of 4.5 ms^{-1} in calculating evaporation but we let u^* and hence mixing depend on the model wind. By doing this, the evaporation term essentially acts as a passive Newtonian cooling and damps the SST toward T^* defined in (2.19). Asymmetric solutions still exist, and their structures shown in Fig. 4 are similar to those shown in Fig. 3. Compared to that in Fig. 3a, the magnitude of the surface winds increases, and presumably compensates for the cooling effect of evaporation south of the equator. The wind-speed-dependent vertical mixing is crucial for maintaining the asymmetric state in this case. When u^* is also replaced by a constant, only a symmetric solution is found.

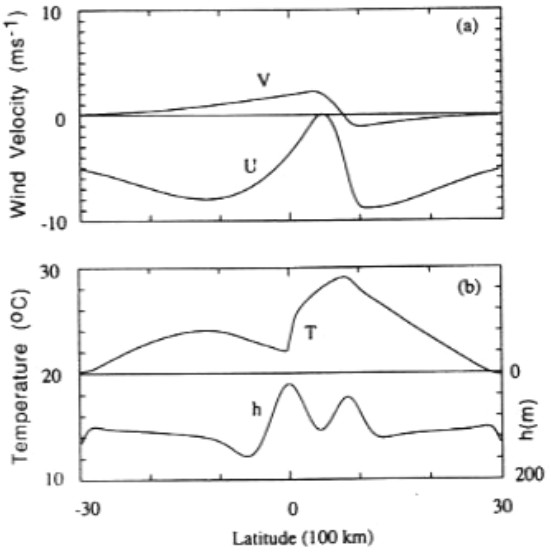

Fig. 4. Same as Fig. 2 but from an experiment where a constant wind speed of 4.5 ms^{-1} is used in the evaporation calculation. Note the difference in the scale of the vertical coordinate for the wind velocity from that in Figs. 2, 3 and 5.

4. Surface evaporation mechanism

In many previous coupled models, the surface heat flux is treated as a Newtonian cooling term. However, the surface latent heat flux also depends on the surface wind speed and can therefore be another mechanism that maintains the asymmetric state. An equatorially asymmetric distribution of the wind speed can cause a large equatorial asymmetry in SST. As an example, we consider a situation in which an ITCZ stays to the north of the equator as in Fig. 3 and that the surface wind speed within the ITCZ is half that at the same latitude on the opposite side of the equator. If we assume that the SST below the ITCZ is 30°C, then, for the latent heat flux to be the same at these two locations*, the SST has to decrease to 19°C south of the equator (see (2.18)).

Since we want to focus on the effect of evaporation, it is convenient to parameterize the ocean dynamics and mixing processes. As seen in the previous section, the main effects of ocean dynamics is to cause upwelling at the equator and to advect cold water away from it. We may therefore specify these effects with a time-invariant function

$$\rho c_p \left(W_e \Delta T + hv \frac{\partial T}{\partial y} \right) = Q_w = Q_w^0 \exp\left[-\frac{1}{2}\left(\frac{y}{R}\right)^2 \right], \tag{4.1}$$

which cools the ocean near the equator. This parameterization mimics the effect of oceanic equatorial upwelling and simplifies our problem. As a result, our ocean model reduces into one single SST equation

$$\frac{\partial T}{\partial t} = \frac{Q_0 - Q_w - C_E^* |U| q_s(T)}{\rho c_p h} + \kappa \frac{\partial^2 T}{\partial y^2}. \tag{4.2}$$

As long as the diffusion term is small, the steady solution to (4.2) is not affected by the depth of the thermocline h. The latter only affects the time scale for the system to adjust to the equilibrium. Therefore, the variation in h is not important here, in contrast to the other extreme case where the wind stirring effect is emphasized. A constant value of $h = 25$ m is thus used in this section. The amplitude of equatorial upwelling Q_w^0 is chosen so that the equilibrium temperature T_E, defined by

$$Q_0 - Q_w - C_E^* U_{\min} q_s(T_E) = 0, \tag{4.3}$$

is 25°C at the equator, 10°C lower than T^*. The sensitivity of the solution to T_E will be investigated at the end of the section. Note that the atmosphere can affect the SST in this model only by changing the surface wind speed in the evaporation formula.

When (4.2) is coupled to the atmosphere, as in the previous section, three steady solutions are found. One of them is symmetric about the equator and the other two are asymmetric. The asymmetric solution with its ITCZ in the northern hemisphere is shown in Fig. 5. The overall features of the asymmetric solution in this much simpler model are very similar to these in Fig. 3. The wind speed dependence is crucial in this case since removing it from (4.2) decouples the ocean from the atmosphere.

As is evident from (4.2), in the steady state, there is a net heat flux into the ocean to balance the cold upwelling near the equator, while outside the equator the net heat flux is small, consistent with heat flux calculations using observed data (Oberhuber, 1988). The heat flux into the ocean is approximately 60 Wm^{-2} at the equator, smaller than the observed. This value however can be increased by increasing the intensity of equatorial upwelling. If we define a "downward" flux in a broad sense as $Q_{\mathrm{down}} = Q_0 - Q_w$ to include the lateral and bottom fluxes, eq. (4.2) actually has the same form as so-called "slab" mixed layer model used in some of the climate studies (Manabe et al., 1975; Hansen et al., 1988). However, the "downward" heat flux in our calculation includes not only the solar radiation but also oceanic upwelling so that it has a minimum at the equator.

The solution in the absence of equatorial upwelling ($Q_w = 0$) is of interest, since it sheds light on the latitude of the off-equatorial ITCZ. Suppose we start with an asymmetric state with high SST off the equator like that in Fig. 5b. A zone of weak winds then forms between the equator and the initial ITCZ. In the absence of equatorial upwelling, the SST in the weak wind zone equatorward of the ITCZ will increase and become

* The observed annual-mean latent heat flux is more or less equatorially symmetric in the tropics (Weare et al., 1981, Esbensen and Kushnir, 1981; Oberhuber, 1988), as is the annual-mean solar radiation.

high enough to cause deep convection. This causes the ITCZ and thus the SST maximum to move equatorward. Fig. 6 shows such an example. Additional experiments show that regardless of its initial location, the ITCZ eventually propagates to the equator. When the center of the ITCZ is on the equator, the wind speed increases with latitude within 10°, lowering the off-equatorial SST. As a result, the solution with an ITCZ at the equator is stable. When there is strong equatorial upwelling, however, the associated cooling prevents the off-equatorial ITCZ propagating into the equator. Fig. 7 depicts the latitude of the ITCZ as a function of the strength of upwelling. The stronger the upwelling, the farther away the ITCZ is from the equator. The ocean dynamics, especially that associated with equatorial upwelling and meridional advection, is important in determining the latitude of the ITCZ. Another interesting point to note in Fig. 7 is that the asymmetric ITCZ solution only occurs in the presence of strong equatorial upwelling. This is consistent with the observation that the permanent northerly ITCZ only exists in the Atlantic and eastern Pacific, where the equatorial upwelling is strong. In the Indian and western Pacific Oceans, the upwelling

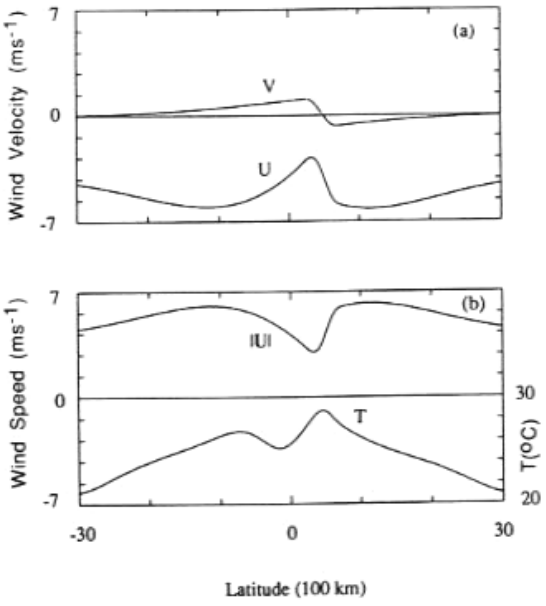

Fig. 5. Meridional distributions of (a) zonal and meridional wind velocities, and (b) wind speed and SST, in an asymmetric solution to the slab mixed-layer model where the depth of the thermocline is fixed as a constant.

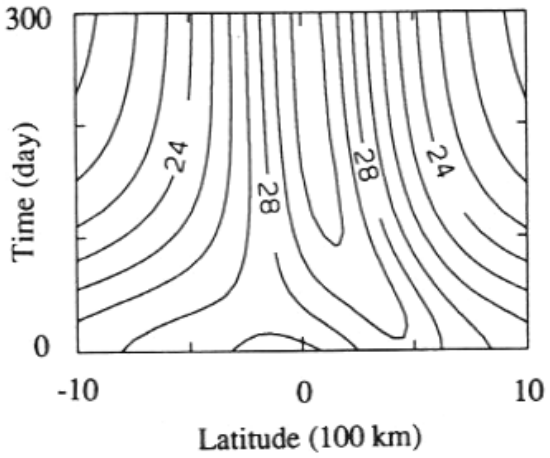

Fig. 6. Latitude-time section of SST in a case with zero equatorial upwelling. The initial condition is the equatorially asymmetric state shown in Fig. 5.

is weak and the warmest SST is found at the equator.

Some non-linearity is necessary to maintain an equatorially asymmetric steady state under the symmetric external conditions. The SST threshold for the deep convection and bulk formula for evaporation used in the model are nonlinear. The nonlinearities in the latter include the product of wind speed and humidity, the minimum wind requirement, and the exponential function in the

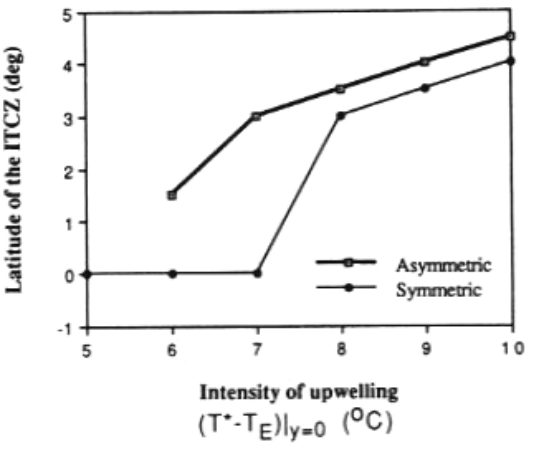

Fig. 7. Latitudes of the ITCZ (maximum in SST) as functions of $(T^* - T_E)|_{y=0}$ (see (2.18) and (4.3) for definition of T^* and T_E), a measure of the intensity of equatorial upwelling.

Clapeyron equation. The bulk formula for evaporation may be linearized as:

$$-|U|\, q_s(T) \approx (U_{eq} + U')\, q_s(T_0) + U_{eq} \frac{dq_s}{dT} T', \tag{4.4}$$

where $T' = T - T_0$. Here, the minimum wind speed requirement is removed, and an assumption is made that the zonal velocity is much larger than the meridional velocity. In a model with this linearized evaporation formula, an asymmetric solution very similar to that shown in Fig. 5 has been obtained (not shown). Therefore, the SST threshold for deep convection, which is observed in the real atmosphere, is the crucial nonlinearity that maintains the asymmetric state in the model.

5. Discussion

This study uses a two-dimensional coupled ocean-atmosphere model to study the processes that can contribute to an equatorially asymmetric state with the ITCZ and warm surface water appearing in only one hemisphere as observed in the Atlantic and eastern Pacific. It has been shown that under permanent equinox condition, the air-sea interactions can develop equatorially asymmetric steady states, with a single ITCZ in only one hemisphere. It may at first seem that mixing processes (and/or evaporation), even in the absence of any dynamical response of the ocean in the form of equatorial upwelling for example, can cause the asymmetry. If the ITCZ initially is at an off-equatorial latitude, say 10° N, then weak winds near 10° N ensure low mixing and hence high surface temperatures there while strong winds elsewhere keep temperatures low so that the ITCZ remains at 10° N. Our model demonstrates that this argument is flawed because, on an equatorial beta-plane, the winds that converge onto the ITCZ are weak on the equatorial side of the ITCZ. The ITCZ therefore moves to the high temperatures closer to the equator until it ultimately is located at the equator. To prevent this and to maintain an asymmetric state, the dynamical response of the ocean, specifically equatorial upwelling induced by the wind, must be taken into account. If that is done, then the mixing processes contribute to the asymmetry. Mixing in the upper layer of the ocean, and evaporation from the surface of the ocean, two processes that depend on the speed of the total wind, play similar roles in contributing to the asymmetry.

The key difference between the eastern Pacific and Atlantic, which have pronounced asymmetries relative to the equator, and the western Pacific and Indian Oceans where convection readily crosses the equator seasonally, is in the mean depth of the thermocline. In the equatorial Pacific Ocean, the zonal variation in the thermocline depth is caused by the prevailing easterly trade winds and by the presence of meridional boundaries. When the thermocline is too deep neither upwelling nor mixing processes can significantly influence sea surface temperatures. That is the case in the western Pacific and Indian Oceans but not in the Atlantic and eastern Pacific. The SST in the warm water pool of the Indian and western Pacific Oceans has a maximum on the equator and is approximately symmetric about the equator, in contrast to that in the Atlantic and eastern Pacific. The location of the ITCZ over the ocean with the western Pacific-type SST profile is a subject currently under debate (Hayashi and Sumi, 1986; Numaguti and Hayashi, 1991; Hess et al., 1992).

On the earth, the sun crosses the equator twice a year. The presence of an annual cycle at the equator in the Atlantic and eastern Pacific is therefore a puzzle because the annual harmonic of solar radiation is virtually zero at the equator. A partial answer to this puzzle is the equatorial asymmetry of the ocean-atmospheric response to time-mean forcing (Xie, 1994). Calculations with our model, which includes a seasonal cycle in solar radiation based on Reed's (1977) formula, shows that the steady asymmetric solutions are stable to this seasonal forcing. The ITCZ stays in one hemisphere throughout the year. SST in our model has an annual cycle at the equator even though the annual solar forcing vanishes there. This happens because the speed of the southerlies and hence the strength of wind stirring have an annual cycle in response to the variation in the northerly ITCZ. This SST annual cycle is a passive response of the ocean through vertical mixing processes and does not require the interactions between the ocean and atmosphere on the equator. In reality, such interactions almost certainly affect the seasonal cycle.

The present study proposes air-sea interaction mechanisms that could maintain an asymmetric ITCZ system even in the absence of any asym-

metric geometry. The asymmetry can favor either hemisphere. In reality the asymmetric geographical features on the earth are presumably crucial in selecting the northern hemisphere for the ITCZ. For example, the tilt of the coastal lines of the American and African Continents relative to a longitude line can cause an equatorial asymmetry in the coastal upwelling. The asymmetry in the land mass distribution between the northern and southern hemispheres can cause asymmetries in the global atmospheric and oceanic circulations. The matter needs further studies.

6. Acknowledgments

The authors would like to thank Y. Hayashi, I. Held, A. Kubokawa, J. Wallace for helpful discussions, and T. Mitchell for his careful reading of the manuscript. During this study, which was funded by a grant from the National Oceanic and Atmospheric Administration (NA26G0102-01), we had the benefit of access to GFDL computer resources. The views expressed herein are those of the authors and do not necessarily reflect the views of NOAA or any of its agencies.

REFERENCES

Anderson, D. L. T. and McCreary, J. P. 1985. Slowly propagating disturbances in a coupled ocean-atmosphere model. *J. Atmos. Sci.* **42**, 615–929.

Charney, J. G. 1969. The intertropical convergence zone and the Hadley circulation of the atmosphere. *Proc. WMO/IUGG Symposium on Numerical weather prediction in Tokyo*, III-73-III-79, Japan Meteor. Agency.

Esbensen, S. K. and Kushnir, V. 1981. The heat budget of the global Ocean: An atlas based on estimates from surface marine observations. *Report* **29**, 27 pp., 188 figs., Clim. Res. Inst., Oreg. State Univ., Corvallis.

Gill, A. E. 1980. Some simple solutions for heat-induced tropical circulation. *Quart. J. Roy. Meteor. Soc.* **106**, 447–462.

Graham, N. E. and Barnett, T. P. 1987. Sea surface temperature, surface wind divergence and convection over tropical oceans. *Science* **238**, 657–659.

Hansen, J. E. et al. 1988. Global climate changes as forecasted by Goddard Institute for Space Studies three-dimension model. *J. Geophys. Res.* **93**, 9341–9364.

Hayashi, Y. Y. and Sumi, A. 1986. The 30–40 day oscillations simulated in an "Aqua Planet" model. *J. Meteor. Soc. Japan* **64**, 451–467.

Herbert, D., Moum, J. N. and Caldwell, D. R. 1991. Does ocean turbulence peak at the equator, revisited. *J. Phys. Oceanogr.* **21**, 1690–1698.

Hess, P. G., Battisti, D. S. and Rasch, P. J. 1993. The maintenance of the intertropical convergence zones and the large-scale tropical circulation on a water-covered earth. *J. Atmos. Sci.* **50**, 691–713.

Hubert, L. F., Krueger, A. F. and Winston, J. S. 1969. The double intertropical convergence zone-Fact or fiction? *J. Atmos. Sci.* **26**, 771–773.

Kornfield, J., Hasler, A. F., Hanson, K. J. and Suomi, V. E. 1967. Photographic cloud climatology from ESSA III and V computer produced mosaics. *Bulletin Amer. Meteor. Soc.* **48**, 878–882.

Kraus, E. B. and Turner, J. S. 1967. A one-dimensional model of the seasonal thermocline. (II). The general theory and its consequences. *Tellus* **19**, 98–109.

Levitus, S. 1982. *Climatological atlas of the world ocean.* NOAA professional paper no. 13, 173 pp. U.S. Government Printing Office, Wahington, DC.

Manabe, S., Hahn, D. G. and Holloway, J. L. Jr. 1974. The seasonal variation of the tropical circulation as simulated by a global model of the atmosphere. *J. Atmos. Sci.* **31**, 43–83.

Manabe, S., Bryan, K. and Spelman, M. J. 1975. A global ocean-atmosphere climate model. Part I. The atmospheric circulation. *J. Phys. Oceanogr.* **5**, 3–29.

Matsuno, T. 1966. Quasi-geostrophic motions in the equatorial area. *J. Meteor. Soc. Japan* **44**, 25–43.

Mitchell, T. P. and Wallace, J. M. 1992. The annual cycle in equatorial convection and sea surface temperature. *J. Climate* **5**, 1140–1156.

Moum, J. N. and Galdwell, D. R. 1985. Local influences on shear-flow turbulence in the equatorial ocean. *Science* **230**, 315–316.

Niiler, P. P. and Kraus, E. B. 1977. One-dimensional models of the upper ocean. *Modeling and prediction of the upper layers of the ocean*, E. B. Kraus, Ed. Pergamon, 143–172.

Numaguti, A. and Hayashi, Y.-Y. 1991. Behaviors of the cumulus activity and the structures of the circulations in the "aqua-planet" model. Part II: Large-scale structures and evaporation-wind feedback. *J. Meteor. Soc. Japan* **69**, 563–579.

Oberhuber, J. M. 1988. An Atlas based on the "COADS" data set: The budgets of heat, buoyancy and turbulent kinetic energy at the surface of the global ocean. *Report no. 15*, 20 pp. + figs. Max-Planck-Institut fur Meteor., Hamburg.

Philander, S. G. H. and Seigel, A. D. 1985. Simulation of El Niño of 1982–1983. *Coupled ocean-atmosphere models*, J. C. J. Nihoul, ed. Elsevier Oceanogr. Series, **40**, Elsevier, 517–541.

Pike, A. C. 1971. Intertropical convergence zone studied

with an interacting atmosphere and ocean model. *Mon. Wea. Rev.* **99**, 469–477.

Rasmusson, E. M. and Carpenter, T. H. 1982. Variations in tropical sea surface temperature and surface wind fields associated with the Southern Oscillation/ El Niño. *Mon. Wea. Rev.* **110**, 354–384.

Reed, R. K. 1977. On estimating insolation over the ocean. *J. Phys. Oceanogr.* **7**, 482–485.

Schopf, P. S. and Cane, M. A. 1983. On equatorial dynamics, mixed layer physics and sea surface temperature. *J. Phys. Oceanogr.* **13**, 917–935.

Wang, B. and Li, T. 1992. A simple tropical atmosphere model of relevance to short-term climate variations. Part I: Model physics. *J. Atmos. Sci.* **50**, 260–284.

Weare, B. C., Strub, P. T. and Samuel, M. D. 1981. Annual mean surface heat fluxes in the tropical Pacific Ocean. *J. Phys. Oceanogr.* **11**, 705–717.

Wright, P. B. 1988. An Atlas based on the "COADS" data set: fields of mean wind, cloudiness and humidity at the surface of the global ocean. *Report no. 14*, 7 pp. + figs., Max-Planck-Institut fur Meteor., Hamburg.

Xie, S.-P., 1994. On the genesis of the equatorial annual cycle. *J. Climate*, in press.

Xie, S.-P., Kubokawa, A. and Hanawa, K. 1989. Oscillations with two feedback processes in a coupled ocean-atmosphere model. *J. Climate* **2**, 946–964.